Advanced Steel Construction – Vol. 19 No. 1 (2023) 17–22
DOI:10.18057/IJASC.2023.19.1.3
(**Special Issue:** *10th International Conference on Advances in Steel Structures, ICASS'2020, Chengdu, China*)

ULTIMATE STRENGTH, DUCTILITY, AND FAILURE MODE OF HIGH-STRENGTH FRICTIONAL BOLTED JOINTS MADE OF HIGH-STRENGTH STEEL

Zi-Ce Qin [1], H. Moriyama [2, *], T. Yamaguchi [3], M. Shigeishi [4], Yu-Yue Xing [1] and A. Hashimoto [5]

[1] *Graduate School of Science and Technology, Kumamoto University, Kumamoto, Japan*
[2] *Graduate School of Technology, Industrial and Social Sciences, Tokushima University, Tokushima, Japan*
[3] *Department of Civil Engineering, Osaka Metropolitan University, Osaka, Japan*
[4] *Department of Civil and Architectural Engineering, Kumamoto University, Kumamoto, Japan*
[5] *Technical Division, Faculty of Engineering, Kumamoto University, Kumamoto, Japan*
* *(Corresponding author: E-mail: moriyama.hitoshi@tokushima-u.ac.jp)*

A B S T R A C T

Further structural rationalization of steel bridges such as weight reduction of members can be realized by using high-strength steel. However, owing to the high yield-to-tensile strength ratio, failure of connected members occurs before the members in the gross area are plastic-deformed sufficiently. In this study, tensile tests of frictional bolted joints with various geometrical configurations and grades of plates and bolts were conducted to compare the failure modes of high-strength and mild steel joints and to investigate the relationship among ultimate strength, ductility, and failure mode. The results indicate that the failure modes of high-strength steel joints were the same as those of mild steel joints and can be almost classified with the respective ratios of net cross-section failure resistance and plate shear failure resistance to bolt shear failure resistance. Ultimate resistance and ductility were maximum in the case of split failure mode where these ratios were approximately 1.0; they increased as the ratios decreased. Therefore, it can be concluded that these ratios should be less than 1.0 to induce the split failure mode to enable the breaking of a high-strength steel joint after the member is plastic-deformed sufficiently.

A R T I C L E H I S T O R Y

Received: 20 July 2022
Revised: 22 August 2022
Accepted: 10 January 2023

K E Y W O R D S

High strength steel;
High-strength frictional bolted joints;
Ultimate strength;
Ductility;
Failure modes

1. Introduction

Further structural rationalization of steel bridges such as weight reduction of members can be realized by using the strength of high-strength steel (hereafter called as HSS) and it improves the productivity and constructability of bridges. However, as the yield-to-tensile strength ratio (hereafter called the yield ratio) of HSS is greater than 0.90, failure of members connected by bolted joints can occur before members in the gross area are sufficiently plastic-deformed. Moreover, Eurocode 3, in which the limit state design is adopted, restricts the yield ratio to 0.72, which restricts the use of HSS [1,2,3]. The resistance relationship of a connected member at a general part and bolted joint part is expressed by eqs. (1)–(3) without considering any partial factors. As shown in these equations for the current design, it is difficult to complete the relationship of HSS members such as truss members, whose axial force is constant in the longitudinal direction.

$$P_{ygd} = A_g \sigma_y \tag{1}$$

$$P_{tnd} = A_n \sigma_t \tag{2}$$

$$P_{ygd} < P_{tnd} \Longleftrightarrow A_g \sigma_y < A_n \sigma_t \Longleftrightarrow \frac{\sigma_y}{\sigma_t} (= YR) < \frac{A_n}{A_g} < 1.0 \tag{3}$$

Here, P_{ygd} is the gross cross-section yield resistance, P_{tnd} is the net cross-section failure resistance, A_g is the gross cross-sectional area, σ_y is the yield strength, A_n is the net cross-sectional area, σ_t is the tensile strength, and YR is the yield ratio.

On the other hand, some researchers report that a HSS joint has the same ductility as a mild steel joint when the connected plate is broken but the bolts are unbroken [4,5,6]. Therefore, if the effect of the yield ratio on the after-slip mechanical behavior is elucidated, structural rationalization with HSS can be realized by controlling the failure mode of the joints and securing the same ductility as a mild steel joint. Recently, a HSS called "steels for bridge high performance structure (SBHS)" was fabricated in Japan; it has high strength and weldability by applying thermos-mechanical control processes [7,8]. Additionally, SBHS has already been specified in Japanese Industrial Standards [9] and various research has been conducted [10,11].

In this study, tensile tests of high-strength frictional bolted joints with SBHS, with various geometrical configurations and grades of steel plate and bolts, were conducted to compare the failure modes of HSS and mild steel joints and to investigate the relationship among ultimate strength, ductility, and failure modes.

2. Tensile tests

2.1. Specimens

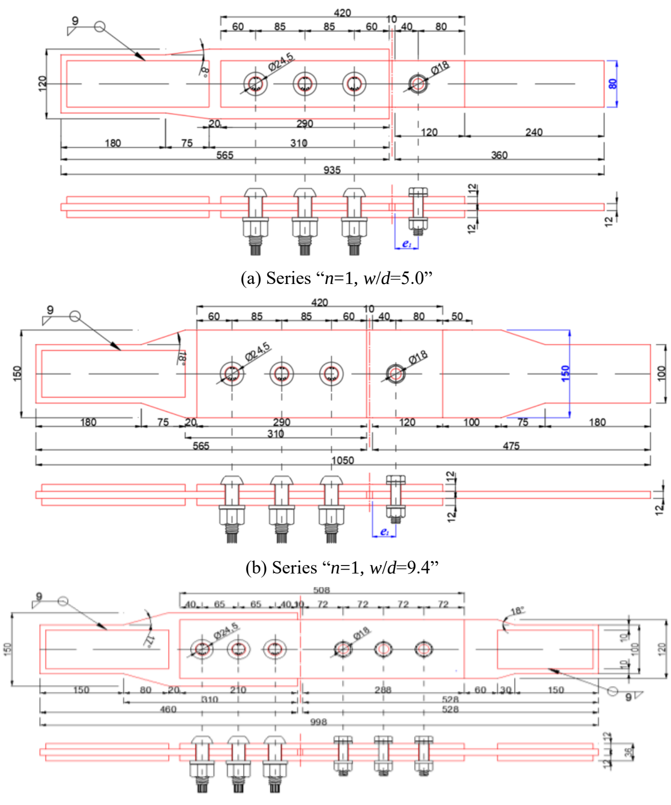

(a) Series "n=1, w/d=5.0"

(b) Series "n=1, w/d=9.4"

(c) Series "n=3"

Fig. 1 Geometrical dimensions of specimens (unit: mm)

Table 1
Structural configurations and bolt arrangement (M16 bolt)

Experimental Case	Number of Bolts	Steel Grade	Bolt Grade	End Distance e_1 (mm)	Bolt Pitch p (mm)	Width w (mm)
n1-B508-ed25-wd50	1	SBHS 500	F8T	40	-	80
n1-B508-ed25-wd94						150
n1-B510-ed25-wd50	1	SBHS 500	F10T	40	-	80
n1-B510-ed25-wd94						150
n1-B510-ed35-wd50				56	-	80
n1-B510-ed35-wd94						150
n1-B512.9-ed35-wd50	1	SBHS 500	12.9 Class	56	-	80
n1-B512.9-ed35-wd94						150
n1-B512-ed25-wd50	1	SBHS 500	12G	40	-	80
n1-B512-ed25-wd94						150
n1-B512-ed35-wd50				56	-	80
n1-B512-ed35-wd94						150
n1-B514-ed25-wd50	1	SBHS 500	S14T	40	-	80
n1-B514-ed25-wd94						150
n1-B514-ed35-wd50				56	-	80
n1-B514-ed35-wd94						150
n1-B710-ed25-wd50	1	SBHS 700	F10T	40	-	80
n1-B710-ed25-wd94						150
n1-B710-ed35-wd50				56	-	80
n1-B710-ed35-wd94						150
n1-B712.9-ed25-wd50	1	SBHS 700	12.9 Class	40	-	80
n1-B712.9-ed25-wd94						150
n1-B712.9-ed35-wd50				56	-	80
n1-B712.9-ed35-wd94						150
n1-B712-ed25-wd50	1	SBHS 700	12G	40	-	80
n1-B712-ed25-wd94						150
n1-B712-ed35-wd50				56	-	80
n1-B712-ed35-wd94						150
n1-B714-ed25-wd50	1	SBHS 700	S14T	40	-	80
n1-B714-ed25-wd94						150
n1-B714-ed35-wd50				56	-	80
n1-B714-ed35-wd94						150
n3-B510-ed45-wd75	3	SBHS 500	F10T	72	72	120
n3-B512-ed45-wd75			12G			
n3-B514-ed45-wd75			S14T			
n3-B712.9-ed45-wd75	3	SBHS 700	12.9 C.	72	72	120
n3-B712-ed45-wd75			12G			
n3-B714-ed45-wd75			S14T			

Fig.1 shows the geometrical dimensions of the specimens. M16 bolts were used on the slip-side because of the limitation of the capacity of the loading machine although it is desirable to use M22 bolts, which are commonly used in steel structures. SHTB-M22 bolts, whose tensile strength is 1400 MPa, were used on the fixed-side.

Table 1 shows the structural configurations and bolt arrangement. As shown in Fig.1 and Table 1, the parameters considered are number of bolts n, steel grades, bolt grades, end distance e_1, and width w. In cases of series "n = 3", structural configurations such as end/edge distance and bolt pitch are not changed. If bolt shear failure occurred and the plastic strain and deformation of connected plate was not confirmed based on the residual stress and bearing deformation after the test, the original bolt hole of cases corresponding to that was expanded to 24.5 mm in diameter to obtain more data by conducting re-tests. Re-tests were conducted with M22 bolts. As shown in Table 2, bolt grades and bolt tensions were varied in the re-test.

Table 2
Structural configurations and bolt arrangement of re-test specimens (M22 bolt)

Experimental Case	Number of Bolts	Steel Grade	Bolt Grade	End Distance e_1 (mm)	Width w (mm)	Designed Bolt Tensions N_d (kN)
n1-B510-ed35-wd50-N100	1	SBHS 500	F10T	56	80	205
n1-B510-ed35-wd50-N150						308
n1-B510-ed35-wd94-N100					150	205
n1-B510-ed35-wd94-N150						308
n1-B710-ed25-wd50-N100	1	SBHS 700	F10T	40	80	205
n1-B710-ed25-wd50-N150						308
n1-B710-ed25-wd94-N100					150	205
n1-B710-ed25-wd94-N150						308
n1-B714-ed35-wd50-N025	1	SBHS 700	S14T	56	80	75
n1-B714-ed35-wd50-N050						150
n1-B714-ed35-wd50-N075						224
n1-B714-ed35-wd50-N100						299
n1-B714-ed35-wd94-N025	1	SBHS 700	S14T	56	150	75
n1-B714-ed35-wd94-N050						150
n1-B714-ed35-wd94-N075						224
n1-B714-ed35-wd94-N100						299

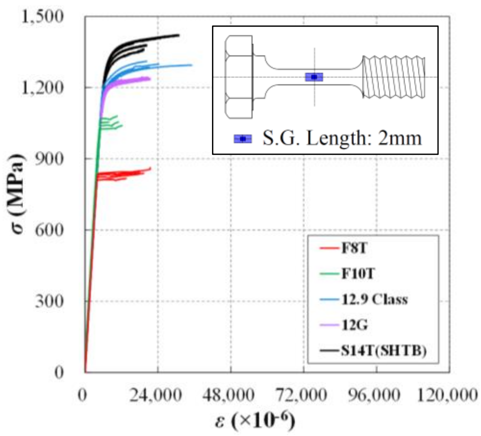

(a) Bolt

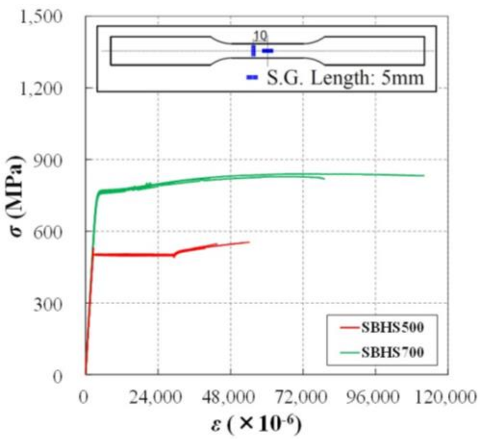

(b) Plate

Fig. 2 Mechanical properties of used steels and bolts based on material tests

Mechanical properties of plates and high-strength bolts obtained by material tests are shown in Table 3 and Fig.2. The number of material test coupons is five in every steel grade and bolt glade. Young's modulus and Poisson's ratio were calculated using the least squares method with strain gauges attached to the bolts at locations illustrated in Fig.2. When a clear yield point was not confirmed because of high yield ratio, 0.2% offset yield strength adopted to calculate the designed yield resistance of all specimens. It can be observed from Table 3 that the yield ratios of all materials are greater than 0.9. The mechanical properties of M22 bolts were quoted from the inspection certificate.

Table 3
Mechanical properties of plates and bolts

Objects	Nominal Thickness t (mm)	Bolt Diameter d (mm)	Steel /Bolt Grade	Nominal Length L (mm)	Young's Modulus E (MPa)	Poisson's Ratio ν	Upper Yield Stress σ_y (MPa)	0.2% Offset Y.S. $\sigma_{y0.2}$ (MPa)	Tensile Strength σ_t (MPa)	Yield Strain $\varepsilon_y = (\sigma_y, \sigma_{y0.2}) / E$ ($\times10^{-6}$)	Yield Ratio $\gamma = (\sigma_y, \sigma_{y0.2}) / \sigma_t$	Elongation after Fracture (%)	Reduction of Area after Fracture (%)
Plate	12	-	SBHS500	-	205,939	0.269	527.4	-	585.4	2,561	0.901	38.6	-
			SBHS700		214,728	0.261	-	765.1	835.5	3,563	0.916	30.6	-
Bolt	-	16	F8T	65	209,623	0.283	829.1	830.2	885.8	3,955	0.936	25.5	73.9
			F10T	65	214,062	0.286	1,050.9	1,047.7	1,093.9	4,909	0.961	21.3	65.5
			12.9 Class	65	212,719	0.283	-	1,215.6	1,307.6	5,714	0.930	15.5	54.7
			12G	75	211,268	0.279	-	1,202.9	1,282.4	5,694	0.938	20.1	56.5
			S14T(SHTB)	75	208,240	0.278	-	1,316.4	1,430.0	6,321	0.921	19.2	54.4
		22*	F10T	75	-	-	-	1,037.0	1,092.0	-	0.950	20.0	71.0
			S14T(SHTB)	75	-	-	-	1,337.0	1,438.0	-	0.930	15.0	54.0

Note: Underlined data is used for calculation of yield strain ε_y and yield ratio γ. The mechanical properties of M22* bolts are quoted from the mill test certificate.

2.2. Designed resistances

Tables 4 and 5 show a summary of the designed resistance of the specimens. The designed slip resistance P_{sd} and net cross-section yield resistance P_{ynd} are calculated using eqs. (4) and (5), respectively. The ratio of these resistances β_d, which is related to the slip behavior, is obtained from eq. (6). The net cross-section failure resistance P_{tnd} and plate shear failure resistance P_{esd} are calculated using eqs. (7) and (8), respectively. The bolt shear resistance P_{bod} is calculated from eq. (9), considering the positional relationship between the shear plane and bolt thread. Only when a 12.9 Class bolt is used, the thread is included in the shear plane.

$$P_{sd} = nm\mu_d N_d \tag{4}$$

$$P_{ynd} = (w - d_0)t_m \times \sigma_y \tag{5}$$

$$\beta_d = \frac{P_{sd}}{P_{ynd}} \tag{6}$$

$$P_{tnd} = (w - d_0)t \times \sigma_t \tag{7}$$

$$P_{esd} = 2 \times \{e_1 + (n-1)p\}t_m \times \frac{\sigma_t}{2} \tag{8}$$

$$P_{bod} = nmA_{b\_sh}\tau_{tb} = n \times 2 \times \frac{\pi d^2}{4} \times \frac{\sigma_{tb}}{\sqrt{3}} \tag{9a}$$

$$P_{bod} = n \times (A_{b\_sh} + A_{b\_th})\tau_{tb} = n \times (A_{b\_sh} + A_{b\_th})\frac{\sigma_{tb}}{\sqrt{3}} \tag{9b}$$

Here, n is the number of bolts, m (=2) is the number of faying surfaces, μ_d (=0.65) is the designed slip coefficient, N_d is the designed bolt tension, w is the width, t_m is the thickness of the connected plate, d_0 is the bolt hole diameter, σ_y is the yield strength of the connected plate, σ_t is the tensile strength of the connected plate, e_1 is the end distance on the slip-side, A_{b_sh} is the effective cross-sectional area of the bolt shank, d is the bolt diameter, A_{b_th} is the effective cross-sectional area of the bolt threaded part, and σ_{tb} is the tensile strength of the bolt. For the re-test, the designed slip coefficient μ_d was set at the minimum 0.20, the coefficient of surfaces as rolled [12], considering the wear of zinc-rich paint coating.

2.3. Measuring items and methods

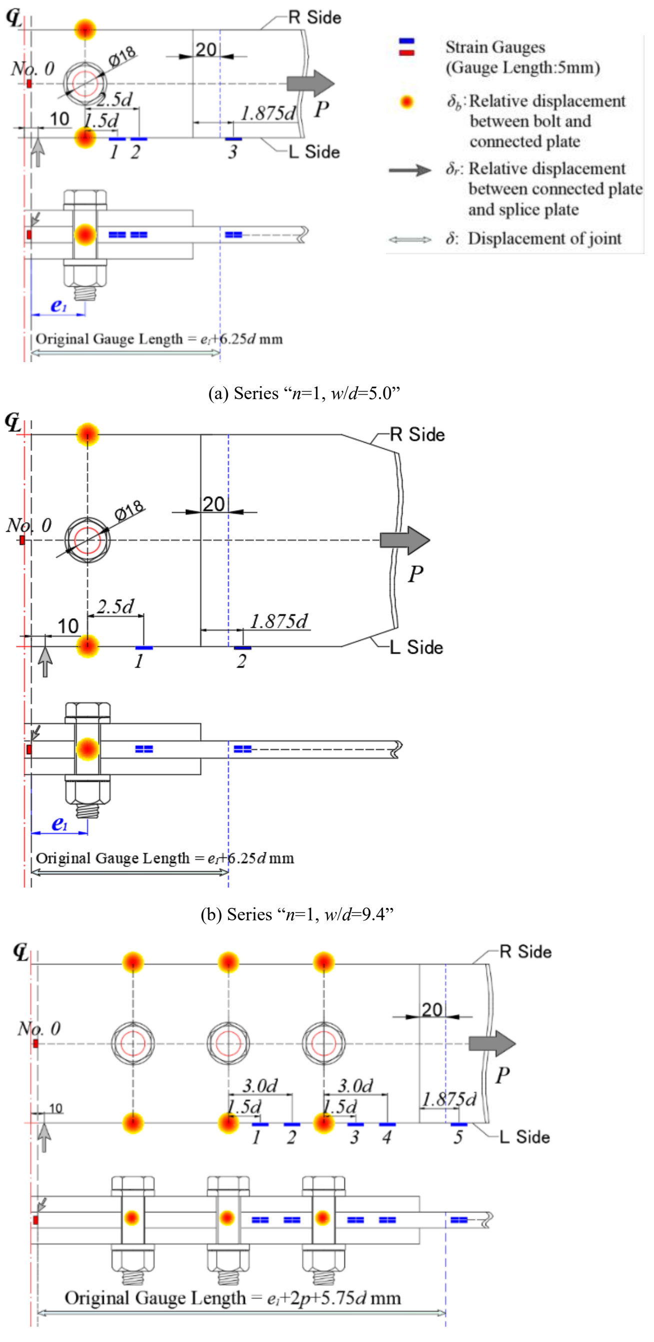

(a) Series "n=1, w/d=5.0"

(b) Series "n=1, w/d=9.4"

(c) Series "n=3"

Fig. 3 Measuring items and their measuring points

Table 4
Designed resistance of the specimens (M16 bolt, $\mu_d = 0.65$)

Experimental Case	P_{sd} (kN)	P_{ynd} (kN)	β_d	P_{bod} (kN)	P_{tnd} (kN)	P_{esd} (kN)	Expected Failure Mode
n1-B508-ed25-wd50	111	392	0.282	206	436	281	BO
n1-B508-ed25-wd94		835	0.133		927		BO
n1-B510-ed25-wd50	138	392	0.351	254	436	281	BO
n1-B510-ed25-wd94		835	0.165		927		BO
n1-B510-ed35-wd50		392	0.351		436	393	BO
n1-B510-ed35-wd94		835	0.162		927		BO
n1-B512.9-ed35-wd50	165	392	0.421	270	436	393	BO
n1-B512.9-ed35-wd94		835	0.198		927		BO
n1-B512-ed25-wd50	173	392	0.441	298	436	281	S
n1-B512-ed25-wd94		835	0.207		927		S
n1-B512-ed35-wd50		392	0.441		436	393	BO
n1-B512-ed35-wd94		835	0.207		927		BO
n1-B514-ed25-wd50	202	392	0.514	332	436	281	S
n1-B514-ed25-wd94		835	0.241		927		S
n1-B514-ed35-wd50		392	0.514		436	393	BO
n1-B514-ed35-wd94		835	0.214		927		BO
n1-B710-ed25-wd50	138	569	0.242	254	622	401	BO
n1-B710-ed25-wd94		1,212	0.114		1,323		BO
n1-B710-ed35-wd50		569	0.242		622	561	BO
n1-B710-ed35-wd94		1,212	0.114		1,323		BO
n1-B712.9-ed25-wd50	165	569	0.291	270	622	401	BO
n1-B712.9-ed25-wd94		1,212	0.136		1,323		BO
n1-B712.9-ed35-wd50		569	0.291		622	561	BO
n1-B712.9-ed35-wd94		1,212	0.136		1,323		BO
n1-B712-ed25-wd50	173	569	0.304	298	622	401	BO
n1-B712-ed25-wd94		1,212	0.143		1,323		BO
n1-B712-ed35-wd50		569	0.304		622	561	BO
n1-B712-ed35-wd94		1212	0.143		1,323		BO
n1-B714-ed25-wd50	202	569	0.354	332	622	401	BO
n1-B714-ed25-wd94		1,212	0.166		1,323		BO
n1-B714-ed35-wd50		569	0.354		622	561	BO
n1-B714-ed35-wd94		1,212	0.166		1,323		BO
n3-B510-ed45-wd75	413	646	0.640	762	716	1,517	N
n3-B512-ed45-wd75	519		0.804	893			N
n3-B514-ed45-wd75	605		0.836	995			N
n3-B712.9-ed45-wd75	496	936	0.530	811	1,023	2,166	BO
n3-B712-ed45-wd75	519		0.554	893			BO
n3-B714-ed45-wd75	605		0.646	995			BO

Fig.3 shows the measuring items and their measuring points. To evaluate the entire behavior of the joint, its displacement and relative displacement between the connected and splice plates were measured. The strain of the side surface of the connected plate was measured to investigate the strain distributions after a major slip. The bolt tension was measured and controlled by the strain gauge attached to the bolt shank. The bolt tension of bolts used in the re-test was controlled by the torque control based on eq. (10). The tightened tensions were 1.1 times the design bolt tensions, considering the creep phenomenon of zinc-rich paint coating after tightening. The relaxation measurement period was more than a week.

$$T = 1.1T_d = 1.1 \times kdN_0 \tag{10}$$

Table 5
Designed resistance of the re-test specimens (M22 bolt, $\mu_d = 0.20$)

Experimental Case	P_{sd} (kN)	P_{ynd} (kN)	β_d	P_{bod} (kN)	P_{tnd} (kN)	P_{esd} (kN)	Expected Failure Mode
n1-B510-ed35-wd50-N100	82	351	0.233	479	390	393	N
n1-B510-ed35-wd50-N150	123		0.350				N
n1-B510-ed35-wd94-N100	82	794	0.103		882	393	S
n1-B510-ed35-wd94-N150	123		0.155				S
n1-B710-ed25-wd50-N100	82	510	0.161	479	556	401	S
n1-B710-ed25-wd50-N150	123		0.241				S
n1-B710-ed25-wd94-N100	82	1,152	0.071		1,258		S
n1-B710-ed25-wd94-N150	123		0.107				S
n1-B714-ed35-wd50-N025	30	510	0.059	631	556	561	S
n1-B714-ed35-wd50-N050	60		0.117				S
n1-B714-ed35-wd50-N075	90		0.176				S
n1-B714-ed35-wd50-N100	120		0.235				S
n1-B714-ed35-wd94-N025	30	1,152	0.026	631	1,258	561	S
n1-B714-ed35-wd94-N050	60		0.052				S
n1-B714-ed35-wd94-N075	90		0.078				S
n1-B714-ed35-wd94-N100	120		0.104				S

Here, T_d is the designed torque, k is the torque coefficient of bolts quoted from the inspection certificate, and d is the bolt diameter.

The applied loading rate was controlled at 1 kN/s by manual operation, as much as practically possible. The sampling time is approximately once per second. In cases of plate failure modes, the applied load was removed at 95% of the maximum load after the peak to observe the peeled area for coating and bearing deformation of the bolt hole. In cases of bolt shear failure mode, loading was continued until bolt breakage occurred due to brittle failure.

3. Results

3.1. Failure modes

As shown in Fig.4, the failure modes confirmed in the test were shear failure (SH), split failure (SP), net cross-section failure (N), bolt shear failure (BO), bolt shear failure and plate shear yielding (BO(SH)), bolt shear failure and net cross-section yielding (BO(N)). These modes are the same as those of mild steel joints [13,14,15], as well as HSS joints in other countries [4,5,6].

Fig.5 shows the definition of failure modes in this paper. Shear failure mode (SH) is the state when only plate shear yielding occurs, followed by tear-out failure. Similarly, for net cross-section failure mode (N) and bolt shear failure mode (BO), only the corresponding yielding and failure occur. Split failure mode (SP) is the state when both plate shear and net cross-section yielding occurs, followed by tear-out failure. The modes BO(SH) and BO(N) induce plate shear yielding and net cross-section yielding, respectively in addition to bolt shear failure. Figs. 4 and 5 show that the zinc-rich paint coating peeled, and the extent of this peeling depended on the plastic area of the connected plate.

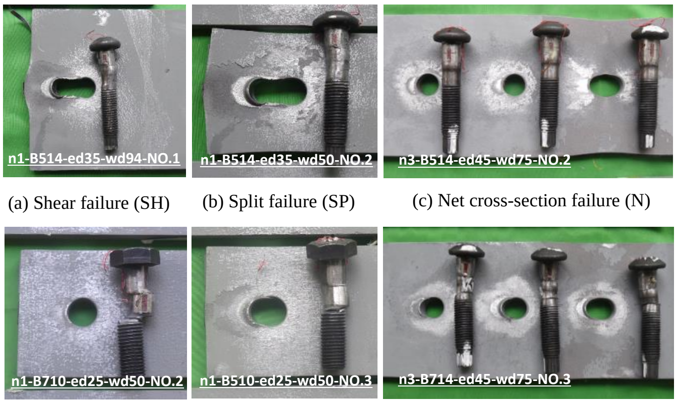

(a) Shear failure (SH) (b) Split failure (SP) (c) Net cross-section failure (N)

(d) Bolt shear failure (BO) (e) Bolt shear failure and plate shear yielding ((BO(SH)) (f) Bolt shear failure and net cross-section yielding ((BO(N))

Fig. 4 Failure modes confirmed in the test

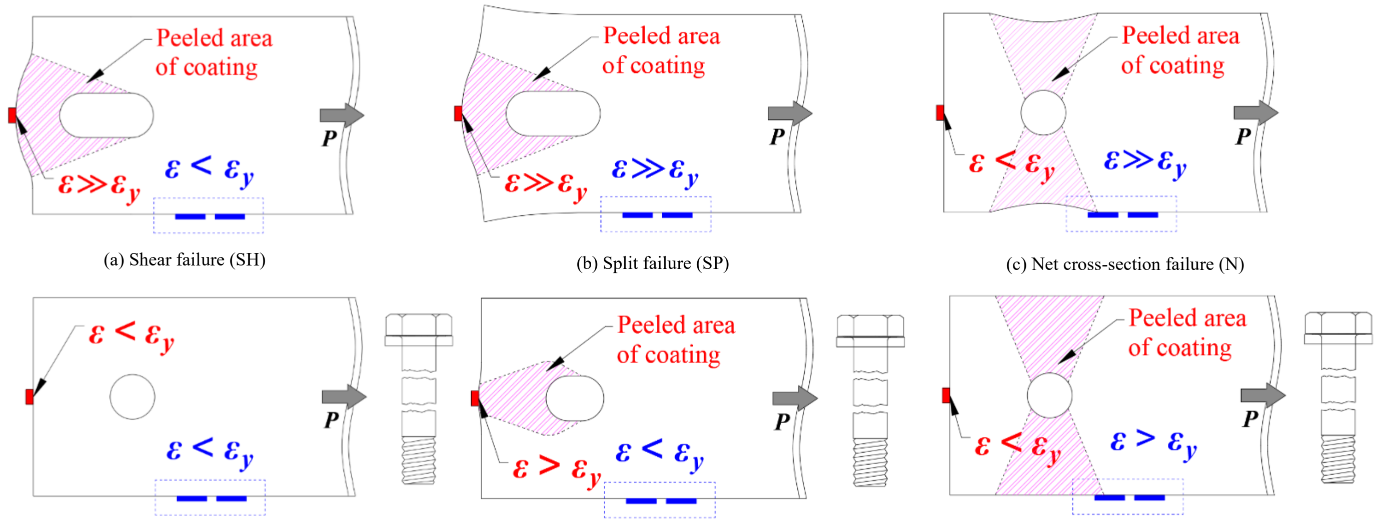

(a) Shear failure (SH) (b) Split failure (SP) (c) Net cross-section failure (N)

(d) Bolt shear failure (BO) (e) Bolt shear failure and plate shear yielding ((BO(SH)) (f) Bolt shear failure and net cross-section yielding ((BO(N))

Fig. 5 Definition of failure modes

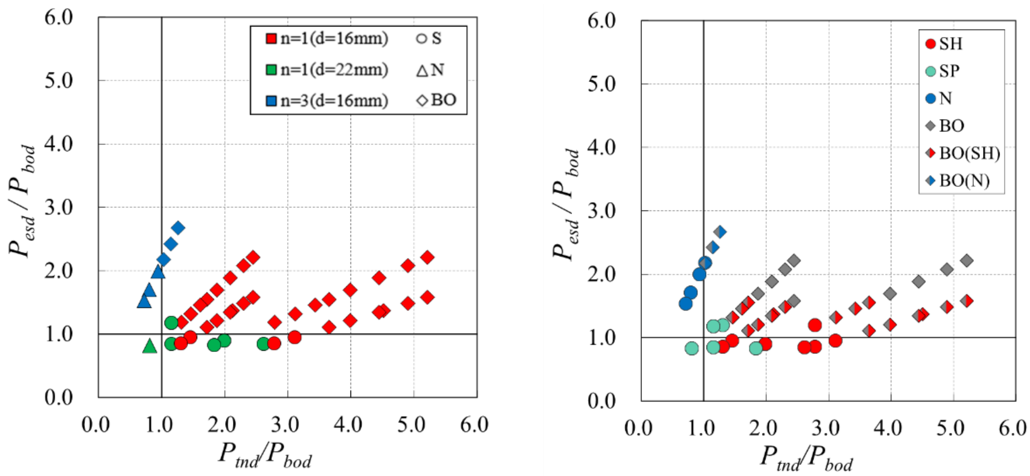

(a) Expected failure modes (b) Actual failure modes

Fig. 6 Classification of the failure modes by P_{tnd}/P_{bod} and P_{esd}/P_{bod}

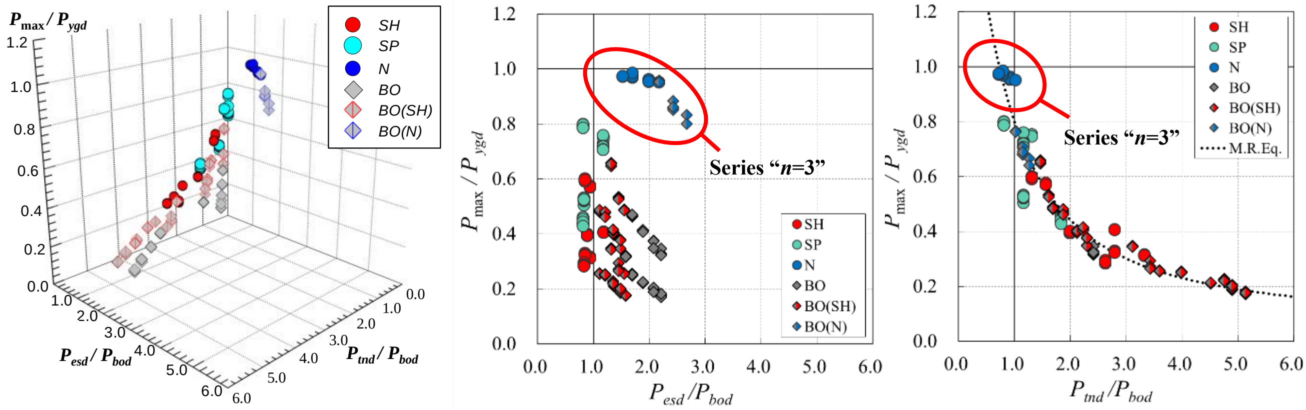

(a) Bird's view (b) P_{max}/P_{ygd} vs P_{esd}/P_{bod} plane (c) P_{max}/P_{ygd} vs P_{tnd}/P_{bod} plane

Fig. 7 Relationship among P_{max}/P_{ygd}, P_{esd}/P_{bod}, and P_{tnd}/P_{bod}

3.2. Comparison of the expected and actual failure modes

The expected and actual failure modes classified by P_{tnd}/P_{bod} and P_{esd}/P_{bod} are shown in Fig.6. Mode SH, N, and BO can be almost classified using the aforementioned conventional equations developed for mild steel joints. Coupled modes such as SP, BO(SH), and BO (N) occurred as P_{tnd}/P_{bod} and P_{esd}/P_{bod} decreased. Especially in the case of SP, P_{esd}/P_{bod} and P_{tnd}/P_{bod} were both approximately 1.0.

3.3. Relationship among ultimate strength, structural configurations, and failure modes

To use the plastic deformation capacity of the connected member, the maximum load of the joint P_{max} must be larger than the gross cross-section yield resistance P_{ygd}. Fig.7 shows the relationship among the ratios P_{max}/P_{ygd}, P_{esd}/P_{bod}, and P_{tnd}/P_{bod}. The maximum load of the joint gradually became larger than the gross cross-section yield resistance as these ratios decreased or the number of bolts increased. In cases of series "$n = 1$", mode SP shows the highest ultimate resistance. However, there is no case in this study whose P_{max}/P_{ygd} is higher than 1.0. Focused on the distribution tendency of the plotted data, P_{max}/P_{ygd} was inversely proportional to P_{esd}/P_{bod}. Therefore, multiple regression analysis was performed to obtain the approximate curve shown in Fig.7(c). The considered approximate equation is expressed as eq. (11). The results of multiple regression analysis are shown in Table 6. The adjusted coefficient of deter-mination R^2_{adj} of this equation is 0.908, indicating a strong correlation.

Table 6
Statistical results of multiple regression analysis

R	R^2	Adjusted R^2_{adj}	Standard Error of the Estimate SE_e	Partial Regression Coefficients	Estimate	95% Confidence Level Lower Limits	95% Confidence Level Upper Limits	Standard Error SE	t-Statistic	P-Statistic
				a	0.051	0.019	0.082	0.016	3.141	0.002
0.953	0.909	0.908	0.07	b	10.006	4.535	15.477	2.770	3.612	0.0004
				c	2.632	1.462	3.802	0.592	4.443	<0.0001

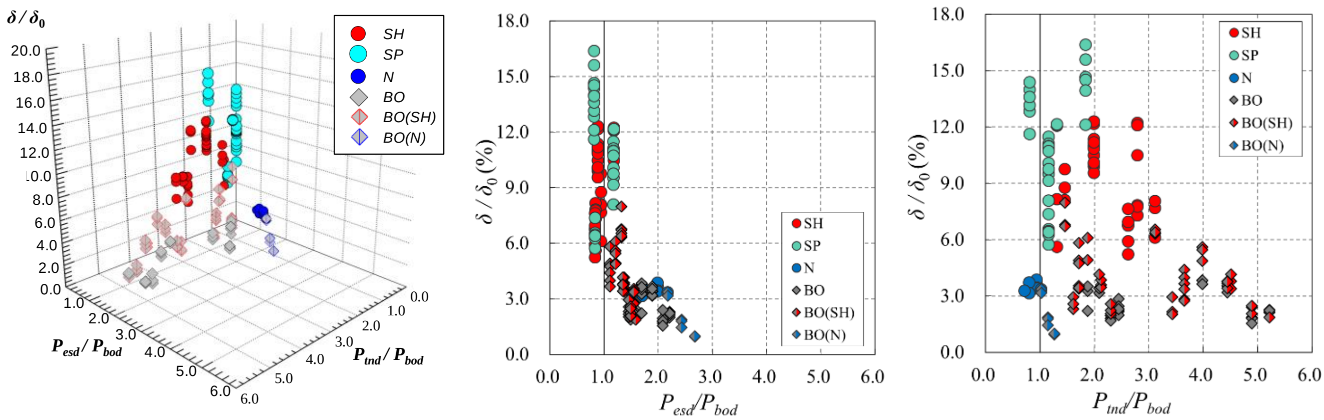

(a) Bird's view (b) δ/δ_0 vs P_{esd}/P_{bod} plane (c) δ/δ_0 vs P_{tnd}/P_{bod} plane

Fig. 8 Relationship among δ/δ_0, P_{esd}/P_{bod}, P_{tnd}/P_{bod}

$$\frac{P_{\max}}{P_{ygd}} = a\exp\left(\frac{b}{P_{tnd}/P_{bod}+c}\right) \tag{11}$$

Here, a, b, and c are partial regression coefficients.

3.4. Relationship among ductility, structural configurations, and failure modes

Similarly, the relationship among elongation δ/δ_0, P_{esd}/P_{bod}, and P_{tnd}/P_{bod} is shown in Fig.8. The elongation δ/δ_0 is the ratio of the entire displacement of the joint at maximum load δ to the original gauge length δ_0. As P_{esd}/P_{bod} and P_{tnd}/P_{bod} decreased, the elongation δ/δ_0 increased. In cases of series "n = 1", mode SP shows the highest ductility and the highest ultimate resistance.

4. Conclusions

In this study, tensile tests of high-strength frictional bolted joints with HSS developed in Japan were conducted to compare the failure modes of HSS and conventional mild steel joints and to investigate the relationship among ultimate strength, ductility, and failure mode. The following conclusions can be drawn.

(1) Failure modes of HSS joints can be assumed to be the same as those of mild steel joints and can be almost classified using the designed ultimate resistance ratios of the plate and bolt such as P_{esd}/P_{bod} and P_{tnd}/P_{bod}, which have already been developed for mild steel joints and widely used in some design codes. For instance, when a coupled failure mode occurred, the corresponding resistance ratio related to the mode was approximately 1.0. Especially, in the case of split failure mode of the connected plate, these ratios were both approximately 1.0.

(2) The maximum load of the joint gradually became larger than the gross cross-section yield resistance these ratios P_{esd}/P_{bod} and P_{tnd}/P_{bod} decreased or the number of bolts increased. There is no case in this paper whose $P_{\max}/P_{ygd}$ is greater than 1.0. As $P_{\max}/P_{ygd}$ was inversely proportional to P_{esd}/P_{bod}, the approximate equation that can precisely estimate $P_{\max}/P_{ygd}$ was obtained, considering only P_{tnd}/P_{bod}. The adjusted coefficient of determination R^2_{adj} of the proposed equation is 0.908.

(3) The entire elongation of the joint δ/δ_0 increased as P_{esd}/P_{bod} and P_{tnd}/P_{bod} decreased and the number of bolts increased along with the maximum load.

(4) In cases of series "n = 1", the split failure mode (SP) exhibits the highest ultimate resistance and ductility. Considering (1)–(3), the ratios P_{esd}/P_{bod} and P_{tnd}/P_{bod} should be less than 1.0 to induce mode SP to enable the breakage of the HSS joint after the member is plastic-deformed sufficiently.

For joints consisting of multiple bolts in the longitudinal and transverse direction, other failure modes such as block shear failure occur easily, which could not be confirmed in this test. Therefore, future work will be devoted to conducting tensile tests on mutiple-bolted joints. Numerical analysis will be also conducted to investigate the influence of various structural configurations and bolt arrangement on the relationship among $P_{\max}/P_{ygd}$, P_{esd}/P_{bod}, and P_{tnd}/P_{bod}.

Acknowledgment

This work was supported by The Japan Iron and Steel Federation. The authors would like to express their gratitude.

References

[1] Eurocode 3: Design of Steel Structures - Part 1-1: General Rules and Rules for Buildings, EN1993-1-1, European Committee for Standardization (CEN), 2005.
[2] Eurocode 3: Design of Steel Structures - Part 1-8: Design of Joints, EN1993-1-8, European Committee for Standardization (CEN), 2005.
[3] Eurocode 3: Design of Steel Structures - Part 1-12: Additional Rules for the Extension of EN 1993 up to Steel Grades S700, EN1993-1-12, European Committee for Standardization (CEN), 2007.
[4] Može P., Beg D. and Lopatic˘ J., "Net cross-section design resistance and local ductility of elements made of high strength steel", Journal of Constructional Steel Research, 63(11), 1431-1441, 2007.
[5] Može P. and Beg D., "High strength steel tension splices with one or two bolts", Journal of Constructional Steel Research, 66(8-9), 1000-1010, 2010.
[6] Wang Y.B., Lyu Y.F., Li G.Q. and Liew J.Y.R., "Behavior of single bolt bearing on high strength steel plate", Journal of Constructional Steel Research, 137, 19-30, 2017.
[7] Homma, K., Tanaka, M., Matsuoka, K., Kasuya, T. and Kawasaki, H., "Development of application technologies for bridge high-performance steel, BHS", Nippon Steel Technical Report, 97, 51-57, 2008.
[8] Miki, C., Ichikawa, A., Kusunoki, T. and Kawabata, F., "Proposal of new high-performance steels for bridges (BHS500, BHS700)", Journal of Japan Society of Civil Engineers, ser. 1, 738(64), 1-10, 2003. (in Japanese)
[9] JIS G 3140: Higher yield strength steel plates for bridges, Japanese Industrial standards, 2011. (in Japanese)
[10] Duc, D.V., Okui, Y., Hagiwara, K. and Nagai, M., "Probabilistic distributions of plate buckling strength for normal and bridge high-performance steels", International Journal of Steel Structures, 13(3), 557-567, 2013.
[11] Rahman, M., Okui, Y., Shoji, T. and Komuro, M., "Probabilistic ultimate buckling strength of stiffened plates, considering thick and high-performance steel", Journal of Constructional Steel Research, 138, 184-195, 2017.
[12] Execution of Steel Structures and Aluminum Structures -Part 2: Technical Requirements for Steel Structures, EN1090-2, European Committee for Standardization (CEN), 2008.
[13] Može P. and Beg D., "A complete study of bearing stress in single bolt connections", Journal of Constructional Steel Research, 95, 126-140, 2014.
[14] Može P., "Bearing strength at bolt holes in connections with large end distance and bolt pitch", Journal of Constructional Steel Research, 147, 132-144, 2018.
[15] Toda Y., Yamaguchi T., Mineyama Y., and Naoe K., "Experimental study of bearing strength of frictional bolted connection based on bolt hole deformation", Journal of Japan Society of Civil Engineers, ser. A1, 70(3), 333-345, 2014. (in Japanese)